sciendo

Acta Materialia Transylvanica 3/2. (2020) 86–89.
DOI: hungarian: https://doi.org/10.33923/amt-2020-02-06
english: https://doi.org/10.33924/amt-2020-02-06

ACTA MATERIALIA TRANSYLVANICA

Experiments with Femtosecond Laser on Monocrystalline Silicon

Anna MALOVECZKY,[1] Márk WINDISCH,[2] Dávid SZABÓ,[3] Gábor BUZA,[4] Dávid UGI,[5] Miklós VERES,[6] István RIGÓ,[7] Péter FÜRJES,[8] Orsolya HAKKEL[9]

[1, 2, 3, 4] *Bay Zoltán Nonprofit Ltd. for Applied Research. Budapest, Hungary, anna.maloveczky@bayzoltan.hu, mark.windisch@bayzoltan.hu, david.szabo2@bayzoltan.hu, gabor.buza@bayzoltan.hu*

[5] *Eötvös Loránd University. Budapest, Hungary, ugidavid42@gmail.com*

[6, 7] *Wigner Research Centre for Physics. Budapest, Hungary, veres.miklos@wigner.mta.hu, rigo.istvan@wigner.mta.hu*

[8, 9] *Centre for Energy Research. Budapest, Hungary, furjes@mfa.kfki.hu, hakkel@energia.mta.hu*

Abstract

Experiments were performed with femtosecond laser on monocrystalline silicon for different application fields. The small focal spot diameter, the ultra-short pulse length, and the high energy density opens new ways in material processing; the treated material will have smaller heat affected zone (HAZ), and allow more precise, higher quality material processing. Micropillars and LIPSS structures were prepared on monocrystalline silicon in our study.

Keywords*: femtosecond laser, surface structuring, micromachining, micropillar.*

1. Introduction

Ultra-short pulsed lasers (i.e., pico- and femtosecond lasers) have undergone rapid development over the past few decades. These lasers have many advantages over conventional (e.g., nanosecond) pulsed lasers. As a result of extremely short pulses, the heat affected zone (HAZ) is much smaller in the treated materials, thus providing high quality micromachining for both ductile and brittle materials. This is because electrons need 1 to 100 ps - depending on the electron-phonon coupling strength of the material being treated - to transfer thermal energy to the nucleus in the lattice. In femtosecond lasers, this results in only a very small fraction of the irradiated energy being transformed into heat.

Another advantage of ultra-short pulsed lasers is that they are capable of generating extremely high peak pulse power, which allows the multi-photon absorption to take place, so that insulating materials (e.g. glass) can be machined with it. Single-photon absorption cannot excite the electrons of the insulating materials into the conduction band. However, due to the high photon density in multi-photon absorption, it is possible to excite the electrons into the conduction band even if the energy of the band gap is greater than that of the photon [1–6].

Because of these characteristics, femtosecond lasers are capable of ablation in high quality. Ablation: during high-power pulsed laser treatment, a plasma cloud of matter exits the material and leaves a well-defined cavity. This process is also called hyper sublimation: the solid enters directly to the plasma phase [1].

Micropillars, microchannels and stents can be machined this way.

Micropillars are used for material research purposes. Plastic deformation works differently at the micro level, and understanding it is important for designing micro-sized parts and developing dislocation theory. In the course of our work, pre-processed micropillars were machined to reduce the time-consuming work with FIB (Focused Ion Beam) [7–11].

Below the ablation threshold, regular, wave-like structures are known as Laser Induced Period-

ic Surface Structures (LIPSS) appear on the surface. The period of these waves is much smaller than the spot diameter of the laser beam. There is no accepted theory for the mechanism of their formation, but probably the interference of incident and backscattered electromagnetic waves and also hydrodynamic phenomena play a role in the formation of these structures. Such structured surfaces can be used, for example, to improve tribological properties, to form antibacterial surfaces, and as a substrate for SERS (Surface Enhanced Raman Scattering) spectroscopy. It is a common problem in Raman spectroscopy that the test component is only present in small amounts in the solution, such as in spinal fluid testing or in detecting drug molecules remaining in filtered water. In this case, the Raman sign of the material is not large enough to detect its presence. A SERS chip (substrate) is then inserted into the Raman microscope. By dropping the test solution to this substrate the Raman signal of the test component can be enhanced up to 1014 fold [12, 13].

The main (electromagnetic) reason for SERS enhancement is: The external electromagnetic field causes the free electrons on the surface of the metals to oscillate: this is a quasi-particle called plasmon. If they have a resonance frequency equal to that of the outer field, then the intensity of the electromagnetic field is amplified. This can mean amplifying the electromagnetic fields of the exciter or the scattered one, or even both[14, 15].

Of course, not only laser beam technology can be used to produce the structures for the uses detailed above, for example, the preparation of a SERS substrate can also be achieved by electrochemical methods. However, laser beam treatments have many advantages: high productivity, repeatability, precision machining and localization [1].

1.1. Laser and investigating devices

The laser source is a Coherent Monaco type resonator. Laser radiation is transmitted without fibres, through mirrors to the z-compensation lens (from Scanlab), then to the galvanic mirrors of the F-theta lens. The repetition rate is adjustable from 188 kHz to 50 MHz, which also allows the equipment to be used in industrial applications. The pulse length is adjustable from 300 fs to 10 ps. The average maximum power is 62 W and the maximum pulse energy is 200 µJ. However, the maximum peak pulse power is 600 MW, which means extremely high energy density. By comparison, the approximate performance of 1 Paks Nuclear Power Plant units is 500 MW. The laser wavelength is 1064 nm and the focal spot diameter is 80 µm.

Images were taken by with a Keyence VHX 2000 microscope a FEI Quanta FEG 3D scanning electron microscope.

Raman spectroscopic investigations were carried out with a Renishaw InVia micro-Raman spectrometer.

1.2 Micropillars

It can take up to a day to prepare one micropillar with FIB. During our work we developed pre-processed micro columns with a femtosecond laser, which was later refined with FIB post-process. With our laser equipment, hundreds of pre-processed micropillars can be made in minutes.

During the preparation of the micro-columns, trenches were made in grid arrangement into monocrystalline silicon. Thus micropillars were formed between the trenches. Pillars with a height of a few tens of micrometres up to a millimetre were formed (see Figures 1, 2).

For the material physics model it is important that the pillar should remain a perfect single crystal. So the presence of a heat affected zone is not allowed. For smaller, 20–60 micrometre high pillars, negligible HAZ were measured with EBSD (Electron Backscatter Diffraction), which can be removed easily and quickly during the FIB post-processing. Larger, hundreds of micrometre-tall pillars have significant, 20–30 micrometres thick HAZ. However, the HAZ can be further reduced in this case by optimizing the parameters of the laser beam treatment: laser power, time between scan repeat, use of refrigerant.

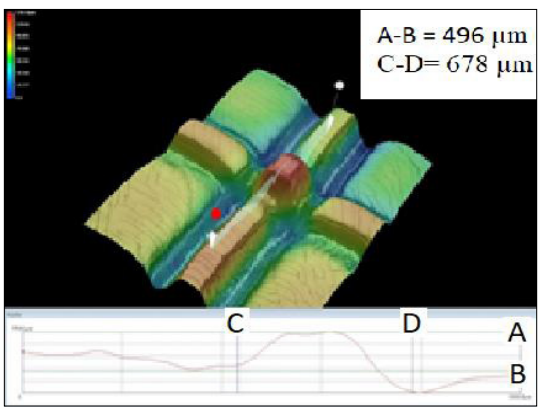

Figure 1. *3D optical microscope image of a 500 micrometre high micropillar and its topographic graph.*

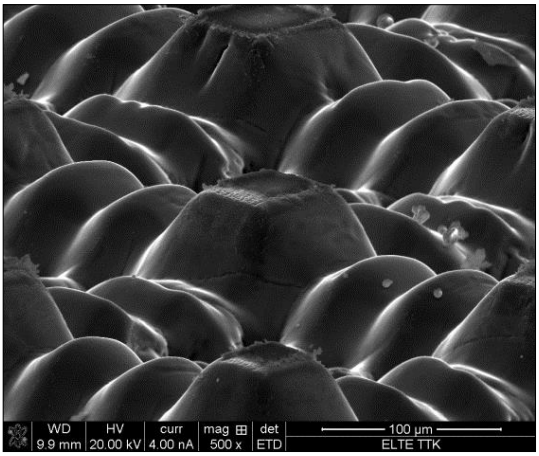

Figure 2. *SEM image of a 50 micrometre high micropillar.*

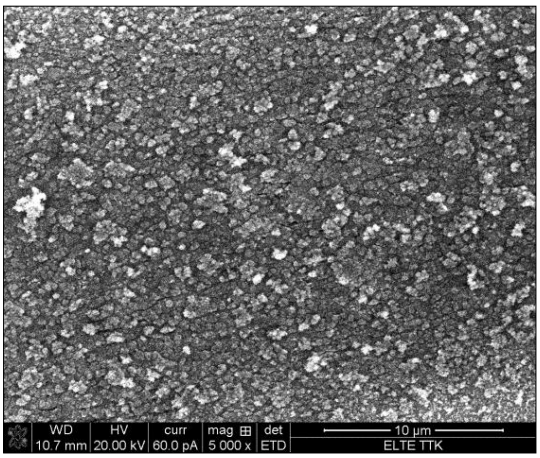

Figure 4. *SEM image of the sample with 360X enhancement factor, without gold coating*

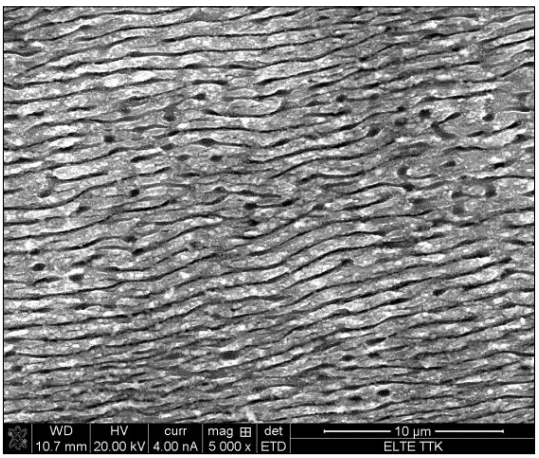

Figure 3. *SEM image of the sample with 360X enhancement factor, without gold coating.*

1.3. LIPSS

If the energy density is close to, but is below the ablation threshold, LIPSS will develop along the scanned lines. The period of the LIPSS is approximately equal to the incident laser's wavelength. The depth and morphology of the LIPSS (and thus its amplification factor) depends on the laser beam parameters used, so in this paper only two representative samples will be introduced (see **Figures 3–4**).

A 150 nm thick gold layer was evaporated onto the LIPSS-structured monocrystalline silicon surface and the enhancement factor was determined using a Raman spectrometer. A sample of benzophenone solution was dropped to the substrate, and the reference signal was measured on a silicon surface with 150 nm gold, but without LIPSS. The enhancement factor was 360X in one case and 490X on the other sample. The exciting laser used in the Raman spectrometer had a wavelength of 610 nm and an exposure time of 1 second.

The two samples differed in their scanning speed: with the scanning speed one magnitude lower, the enhancement factor was higher. Increasing the enhancement factor is favoured by a homogeneous structure composed of several small particles, which can be achieved by slower scanning.

2. Conclusion

In the course of our work we have created different surfaces on a monocrystalline silicon with a femtosecond laser.

Femtosecond laser machining of the pre-processed micropillars significantly reduced machining time with FIB, but further optimization of the laser parameters is desirable to reduce the HAZ.

LIPSS made by us with 150 nm gold coating greatly enhances the Raman signal of benzophenone. We plan to increase the enhancement factor further and to perform measurements with other sample molecules and excitation wavelengths.

We also plan to investigate the tribological performance of the surfaces with LIPSS.

References

[1] Mangirdas M., Albertas Ž., Satoshi H., Yoshio H., Vygantas M., Ričardas B., Saulius J.: *Ultrafast laser processing of materials: from science to industry.* Light: Science & Applications, 5. (2016) 16–133.

[2] Mathis A., Courvoisiera F., Froehly L., Furfaro L., Jacquot M., Lacourt P. A., Dudley J. M.: *Micromachining along a curve. Femtosecond laser mi-*

cromachining of curved profiles in diamond and silicon using accelerating beams. Applied Physics Letters, 101. (2012) 71–110. https://doi.org/10.1063/1.4745925

[3] Evgeny L.: *Mechanisms of femtosecond LIPSS formation induced by periodic surface temperature modulation.* Applied Surface Science, 374. (2016) 30.

[4] Kaiwen D., Cong W., Yu Z., Zheng X., Zhi L., Shu M., Biwei W.: *One-step fabrication of multifunctional fusiform hierarchical micro/nanostructures on copper by femtosecond laser*. Surface and Coatings Technology, 367. (2019) 244–251. https://doi.org/10.1016/j.surfcoat.2019.04.005

[5] Rafael R. G., Eric M.: *Femtosecond laser micromachining in transparent materials*. Nature Photonics, 2. (2008) 219–225.

[6] Andrius M., Saulius J., Mitsuru W., Masafumi M., Shigeki M., Hiroaki M., Junji N.: *Femtosecond laser-assisted three-dimensional microfabrication in silica*. Optics Letters, 26/5. (2001) 277–279. https://doi.org/10.1364/OL.26.000277

[7] Akarapu S., Zbib H. M., Bahr D. F.: *Analysis of heterogeneous deformation and dislocation dynamics in single crystal micropillars under compression.* International Journal of Plasticity, 26/2. (2010) 239–257. https://doi.org/10.1016/j.ijplas.2009.06.005

[8] Aifantis E. C.: *Gradient Deformation Models at Nano, Micro, and Macro Scales*. Journal of Engineering Materials and Technology, 121/2. (1999) 189–202.

[9] Eduardo B.: *Interpretation of the size effects in micropillar compression by a strain gradient crystal plasticity theory*. International Journal of Plasticity, 116. (2019) 31. https://doi.org/10.1016/j.ijplas.2019.01.011

[10] Tanga H., Schwarzb K. W., Espinosaa H. D.: *Dislocation escape-related size effects in single-crystal micropillars under uniaxial compression*. Acta Materialia, 55/5. (2007) 1607–1616. https://doi.org/10.1016/j.actamat.2006.10.021

[11] William D., Nix Seok W. L.: *Micro-pillar plasticity controlled by dislocation nucleation at surfaces.* Philosophical Magazine, 91/7–9. (2011) 1084–1096. https://doi.org/10.1080/14786435.2010.502141

[12] Jijo E. G., Unnikrishnan V. K., Deepak M., Santhosh C., Sajan D. G.: *Flexible Superhydrophobic SERS Substrates Fabricated by In Situ Reduction of Ag on Femtosecond Laser-Written Hierarchical Surfaces*. Sensors and Actuators B, 272/1. (2018) 485–493. https://doi.org/10.1016/j.snb.2018.05.155

[13] Steven E. J. B., Narayana M. S. S.: *Surface-Enhanced Raman Spectroscopy (SERS) for Sub-Micromolar Detection of DNA/RNA Mononucleotides*. Journal of the American Chemical Society, 128/49. (2006) 15580–15581. https://doi.org/10.1021/ja066263w

[14] Ximei Q., Jun L., Shuming N.: S*timuli-Responsive SERS Nanoparticles. Conformational Control of Plasmonic Coupling and Surface Raman Enhancement*. Journal of the American Chemical Society, 131/22. (2009) 7540–7541. https://doi.org/10.1021/ja902226z

[15] Zhu Z., Yan Z., Zhan P., Wang Z.: *Large-area surface-enhanced Raman scattering-active substrates fabricated by femtosecond laser ablation*. Science China Physics, Mechanics and Astronomy, 56. (2013) 1806–1809.